

Measurement of the Hadronic Form Factors in $D_s^+ \rightarrow \phi e^+ \nu_e$ Decays

The *BABAR* Collaboration

October 15, 2018

Abstract

Based on the measured four-dimensional rate for $D_s^+ \rightarrow \phi e^+ \nu_e$ decays, we have determined the ratios of the three hadronic form factors,

$$r_V = V(0)/A_1(0) = 1.636 \pm 0.067 \pm 0.038 \text{ and } r_2 = A_2(0)/A_1(0) = 0.705 \pm 0.056 \pm 0.029,$$

using a simple pole ansatz for the q^2 dependence, with fixed values of the pole masses for both the vector and axial form factors. By a separate fit to the same data, we have also extracted the pole mass for the axial form factors, m_A :

$$r_V = V(0)/A_1(0) = 1.633 \pm 0.081 \pm 0.068, \quad r_2 = A_2(0)/A_1(0) = 0.711 \pm 0.111 \pm 0.096 \\ \text{and } m_A = (2.53_{-0.35}^{+0.54} \pm 0.54) \text{GeV}/c^2.$$

Submitted to the 33rd International Conference on High-Energy Physics, ICHEP 06,
26 July—2 August 2006, Moscow, Russia.

Stanford Linear Accelerator Center, Stanford University, Stanford, CA 94309

Work supported in part by Department of Energy contract DE-AC03-76SF00515.

The BABAR Collaboration,

B. Aubert, R. Barate, M. Bona, D. Boutigny, F. Couderc, Y. Karyotakis, J. P. Lees, V. Poireau,
V. Tisserand, A. Zghiche

*Laboratoire de Physique des Particules, IN2P3/CNRS et Université de Savoie, F-74941 Annecy-Le-Vieux,
France*

E. Grauges

Universitat de Barcelona, Facultat de Física, Departament ECM, E-08028 Barcelona, Spain

A. Palano

Università di Bari, Dipartimento di Fisica and INFN, I-70126 Bari, Italy

J. C. Chen, N. D. Qi, G. Rong, P. Wang, Y. S. Zhu

Institute of High Energy Physics, Beijing 100039, China

G. Eigen, I. Ofte, B. Stugu

University of Bergen, Institute of Physics, N-5007 Bergen, Norway

G. S. Abrams, M. Battaglia, D. N. Brown, J. Button-Shafer, R. N. Cahn, E. Charles, M. S. Gill,
Y. Groysman, R. G. Jacobsen, J. A. Kadyk, L. T. Kerth, Yu. G. Kolomensky, G. Kukartsev, G. Lynch,
L. M. Mir, T. J. Orimoto, M. Pripstein, N. A. Roe, M. T. Ronan, W. A. Wenzel

Lawrence Berkeley National Laboratory and University of California, Berkeley, California 94720, USA

P. del Amo Sanchez, M. Barrett, K. E. Ford, A. J. Hart, T. J. Harrison, C. M. Hawkes, S. E. Morgan,
A. T. Watson

University of Birmingham, Birmingham, B15 2TT, United Kingdom

T. Held, H. Koch, B. Lewandowski, M. Pelizaeus, K. Peters, T. Schroeder, M. Steinke
Ruhr Universität Bochum, Institut für Experimentalphysik 1, D-44780 Bochum, Germany

J. T. Boyd, J. P. Burke, W. N. Cottingham, D. Walker

University of Bristol, Bristol BS8 1TL, United Kingdom

D. J. Asgeirsson, T. Cuhadar-Donszelmann, B. G. Fulsom, C. Hearty, N. S. Knecht, T. S. Mattison,
J. A. McKenna

University of British Columbia, Vancouver, British Columbia, Canada V6T 1Z1

A. Khan, P. Kyberd, M. Saleem, D. J. Sherwood, L. Teodorescu

Brunel University, Uxbridge, Middlesex UB8 3PH, United Kingdom

V. E. Blinov, A. D. Bukin, V. P. Druzhinin, V. B. Golubev, A. P. Onuchin, S. I. Serednyakov,
Yu. I. Skovpen, E. P. Solodov, K. Yu Todyshev

Budker Institute of Nuclear Physics, Novosibirsk 630090, Russia

D. S. Best, M. Bondioli, M. Bruinsma, M. Chao, S. Curry, I. Eschrich, D. Kirkby, A. J. Lankford, P. Lund,
M. Mandelkern, R. K. Mommsen, W. Roethel, D. P. Stoker

University of California at Irvine, Irvine, California 92697, USA

S. Abachi, C. Buchanan

University of California at Los Angeles, Los Angeles, California 90024, USA

S. D. Foulkes, J. W. Gary, O. Long, B. C. Shen, K. Wang, L. Zhang
University of California at Riverside, Riverside, California 92521, USA

H. K. Hadavand, E. J. Hill, H. P. Paar, S. Rahatlou, V. Sharma
University of California at San Diego, La Jolla, California 92093, USA

J. W. Berryhill, C. Campagnari, A. Cunha, B. Dahmes, T. M. Hong, D. Kovalskyi, J. D. Richman
University of California at Santa Barbara, Santa Barbara, California 93106, USA

T. W. Beck, A. M. Eisner, C. J. Flacco, C. A. Heusch, J. Kroseberg, W. S. Lockman, G. Nesom, T. Schalk,
B. A. Schumm, A. Seiden, P. Spradlin, D. C. Williams, M. G. Wilson
University of California at Santa Cruz, Institute for Particle Physics, Santa Cruz, California 95064, USA

J. Albert, E. Chen, A. Dvoretzkii, F. Fang, D. G. Hitlin, I. Narsky, T. Piatenko, F. C. Porter, A. Ryd,
A. Samuel
California Institute of Technology, Pasadena, California 91125, USA

G. Mancinelli, B. T. Meadows, K. Mishra, M. D. Sokoloff
University of Cincinnati, Cincinnati, Ohio 45221, USA

F. Blanc, P. C. Bloom, S. Chen, W. T. Ford, J. F. Hirschauer, A. Kreisel, M. Nagel, U. Nauenberg,
A. Olivas, W. O. Ruddick, J. G. Smith, K. A. Ulmer, S. R. Wagner, J. Zhang
University of Colorado, Boulder, Colorado 80309, USA

A. Chen, E. A. Eckhart, A. Soffer, W. H. Toki, R. J. Wilson, F. Winklmeier, Q. Zeng
Colorado State University, Fort Collins, Colorado 80523, USA

D. D. Altenburg, E. Feltresi, A. Hauke, H. Jasper, J. Merkel, A. Petzold, B. Spaan
Universität Dortmund, Institut für Physik, D-44221 Dortmund, Germany

T. Brandt, V. Klose, H. M. Lacker, W. F. Mader, R. Nogowski, J. Schubert, K. R. Schubert, R. Schwierz,
J. E. Sundermann, A. Volk
Technische Universität Dresden, Institut für Kern- und Teilchenphysik, D-01062 Dresden, Germany

D. Bernard, G. R. Bonneaud, E. Latour, Ch. Thiebaux, M. Verderi
Laboratoire Leprince-Ringuet, CNRS/IN2P3, Ecole Polytechnique, F-91128 Palaiseau, France

P. J. Clark, W. Gradl, F. Muheim, S. Playfer, A. I. Robertson, Y. Xie
University of Edinburgh, Edinburgh EH9 3JZ, United Kingdom

M. Andreotti, D. Bettoni, C. Bozzi, R. Calabrese, G. Cibinetto, E. Luppi, M. Negrini, A. Petrella,
L. Piemontese, E. Prencipe
Università di Ferrara, Dipartimento di Fisica and INFN, I-44100 Ferrara, Italy

F. Anulli, R. Baldini-Ferrolì, A. Calcaterra, R. de Sangro, G. Finocchiaro, S. Pacetti, P. Patteri,
I. M. Peruzzi,¹ M. Piccolo, M. Rama, A. Zallo
Laboratori Nazionali di Frascati dell'INFN, I-00044 Frascati, Italy

¹Also with Università di Perugia, Dipartimento di Fisica, Perugia, Italy

A. Buzzo, R. Capra, R. Contri, M. Lo Vetere, M. M. Macri, M. R. Monge, S. Passaggio, C. Patrignani,
E. Robutti, A. Santroni, S. Tosi

Università di Genova, Dipartimento di Fisica and INFN, I-16146 Genova, Italy

G. Brandenburg, K. S. Chaisanguanthum, M. Morii, J. Wu

Harvard University, Cambridge, Massachusetts 02138, USA

R. S. Dubitzky, J. Marks, S. Schenk, U. Uwer

Universität Heidelberg, Physikalisches Institut, Philosophenweg 12, D-69120 Heidelberg, Germany

D. J. Bard, W. Bhimji, D. A. Bowerman, P. D. Dauncey, U. Egede, R. L. Flack, J. A. Nash,
M. B. Nikolich, W. Panduro Vazquez

Imperial College London, London, SW7 2AZ, United Kingdom

P. K. Behera, X. Chai, M. J. Charles, U. Mallik, N. T. Meyer, V. Ziegler

University of Iowa, Iowa City, Iowa 52242, USA

J. Cochran, H. B. Crawley, L. Dong, V. Eyges, W. T. Meyer, S. Prell, E. I. Rosenberg, A. E. Rubin

Iowa State University, Ames, Iowa 50011-3160, USA

A. V. Gritsan

Johns Hopkins University, Baltimore, Maryland 21218, USA

A. G. Denig, M. Fritsch, G. Schott

Universität Karlsruhe, Institut für Experimentelle Kernphysik, D-76021 Karlsruhe, Germany

N. Arnaud, M. Davier, G. Grosdidier, A. Höcker, F. Le Diberder, V. Lepeltier, A. M. Lutz, A. Oyanguren,
S. Pruvot, S. Rodier, P. Roudeau, M. H. Schune, A. Stocchi, W. F. Wang, G. Wormser

*Laboratoire de l'Accélérateur Linéaire, IN2P3/CNRS et Université Paris-Sud 11, Centre Scientifique
d'Orsay, B.P. 34, F-91898 ORSAY Cedex, France*

C. H. Cheng, D. J. Lange, D. M. Wright

Lawrence Livermore National Laboratory, Livermore, California 94550, USA

C. A. Chavez, I. J. Forster, J. R. Fry, E. Gabathuler, R. Gamet, K. A. George, D. E. Hutchcroft,
D. J. Payne, K. C. Schofield, C. Touramanis

University of Liverpool, Liverpool L69 7ZE, United Kingdom

A. J. Bevan, F. Di Lodovico, W. Menges, R. Sacco

Queen Mary, University of London, E1 4NS, United Kingdom

G. Cowan, H. U. Flaecher, D. A. Hopkins, P. S. Jackson, T. R. McMahon, S. Ricciardi, F. Salvatore,
A. C. Wren

*University of London, Royal Holloway and Bedford New College, Egham, Surrey TW20 0EX, United
Kingdom*

D. N. Brown, C. L. Davis

University of Louisville, Louisville, Kentucky 40292, USA

J. Allison, N. R. Barlow, R. J. Barlow, Y. M. Chia, C. L. Edgar, G. D. Lafferty, M. T. Naisbit,
J. C. Williams, J. I. Yi

University of Manchester, Manchester M13 9PL, United Kingdom

C. Chen, W. D. Hulsbergen, A. Jawahery, C. K. Lae, D. A. Roberts, G. Simi

University of Maryland, College Park, Maryland 20742, USA

G. Blaylock, C. Dallapiccola, S. S. Hertzbach, X. Li, T. B. Moore, S. Saremi, H. Staengle

University of Massachusetts, Amherst, Massachusetts 01003, USA

R. Cowan, G. Sciolla, S. J. Sekula, M. Spitznagel, F. Taylor, R. K. Yamamoto

*Massachusetts Institute of Technology, Laboratory for Nuclear Science, Cambridge, Massachusetts 02139,
USA*

H. Kim, S. E. McLachlin, P. M. Patel, S. H. Robertson

McGill University, Montréal, Québec, Canada H3A 2T8

A. Lazzaro, V. Lombardo, F. Palombo

Università di Milano, Dipartimento di Fisica and INFN, I-20133 Milano, Italy

J. M. Bauer, L. Cremaldi, V. Eschenburg, R. Godang, R. Kroeger, D. A. Sanders, D. J. Summers,
H. W. Zhao

University of Mississippi, University, Mississippi 38677, USA

S. Brunet, D. Côté, M. Simard, P. Taras, F. B. Viaud

Université de Montréal, Physique des Particules, Montréal, Québec, Canada H3C 3J7

H. Nicholson

Mount Holyoke College, South Hadley, Massachusetts 01075, USA

N. Cavallo,² G. De Nardo, F. Fabozzi,³ C. Gatto, L. Lista, D. Monorchio, P. Paolucci, D. Piccolo,
C. Sciacca

Università di Napoli Federico II, Dipartimento di Scienze Fisiche and INFN, I-80126, Napoli, Italy

M. A. Baak, G. Raven, H. L. Snoek

*NIKHEF, National Institute for Nuclear Physics and High Energy Physics, NL-1009 DB Amsterdam, The
Netherlands*

C. P. Jessop, J. M. LoSecco

University of Notre Dame, Notre Dame, Indiana 46556, USA

T. Allmendinger, G. Benelli, L. A. Corwin, K. K. Gan, K. Honscheid, D. Hufnagel, P. D. Jackson,
H. Kagan, R. Kass, A. M. Rahimi, J. J. Regensburger, R. Ter-Antonyan, Q. K. Wong

Ohio State University, Columbus, Ohio 43210, USA

N. L. Blount, J. Brau, R. Frey, O. Igonkina, J. A. Kolb, M. Lu, R. Rahmat, N. B. Sinev, D. Strom,
J. Strube, E. Torrence

University of Oregon, Eugene, Oregon 97403, USA

²Also with Università della Basilicata, Potenza, Italy

³Also with Università della Basilicata, Potenza, Italy

A. Gaz, M. Margoni, M. Morandin, A. Pompili, M. Posocco, M. Rotondo, F. Simonetto, R. Stroili, C. Voci
Università di Padova, Dipartimento di Fisica and INFN, I-35131 Padova, Italy

M. Benayoun, H. Briand, J. Chauveau, P. David, L. Del Buono, Ch. de la Vaissière, O. Hamon,
B. L. Hartfiel, M. J. J. John, Ph. Leruste, J. Malcès, J. Ocariz, L. Roos, G. Therin
*Laboratoire de Physique Nucléaire et de Hautes Energies, IN2P3/CNRS, Université Pierre et Marie
Curie-Paris6, Université Denis Diderot-Paris7, F-75252 Paris, France*

L. Gladney, J. Panetta
University of Pennsylvania, Philadelphia, Pennsylvania 19104, USA

M. Biasini, R. Covarelli
Università di Perugia, Dipartimento di Fisica and INFN, I-06100 Perugia, Italy

C. Angelini, G. Batignani, S. Bettarini, F. Bucci, G. Calderini, M. Carpinelli, R. Cenci, F. Forti,
M. A. Giorgi, A. Lusiani, G. Marchiori, M. A. Mazur, M. Morganti, N. Neri, E. Paoloni, G. Rizzo,
J. J. Walsh
Università di Pisa, Dipartimento di Fisica, Scuola Normale Superiore and INFN, I-56127 Pisa, Italy

M. Haire, D. Judd, D. E. Wagoner
Prairie View A&M University, Prairie View, Texas 77446, USA

J. Biesiada, N. Danielson, P. Elmer, Y. P. Lau, C. Lu, J. Olsen, A. J. S. Smith, A. V. Telnov
Princeton University, Princeton, New Jersey 08544, USA

F. Bellini, G. Cavoto, A. D'Orazio, D. del Re, E. Di Marco, R. Faccini, F. Ferrarotto, F. Ferroni,
M. Gaspero, L. Li Gioi, M. A. Mazzoni, S. Morganti, G. Piredda, F. Polci, F. Safai Tehrani, C. Voena
Università di Roma La Sapienza, Dipartimento di Fisica and INFN, I-00185 Roma, Italy

M. Ebert, H. Schröder, R. Waldi
Universität Rostock, D-18051 Rostock, Germany

T. Adye, N. De Groot, B. Franek, E. O. Olaiya, F. F. Wilson
Rutherford Appleton Laboratory, Chilton, Didcot, Oxon, OX11 0QX, United Kingdom

R. Aleksan, S. Emery, A. Gaidot, S. F. Ganzhur, G. Hamel de Monchenault, W. Kozanecki, M. Legendre,
G. Vasseur, Ch. Yèche, M. Zito
DSM/Daphnia, CEA/Saclay, F-91191 Gif-sur-Yvette, France

X. R. Chen, H. Liu, W. Park, M. V. Purohit, J. R. Wilson
University of South Carolina, Columbia, South Carolina 29208, USA

M. T. Allen, D. Aston, R. Bartoldus, P. Bechtle, N. Berger, R. Claus, J. P. Coleman, M. R. Convery,
M. Cristinziani, J. C. Dingfelder, J. Dorfan, G. P. Dubois-Felsmann, D. Dujmic, W. Dunwoodie,
R. C. Field, T. Glanzman, S. J. Gowdy, M. T. Graham, P. Grenier,⁴ V. Halyo, C. Hast, T. Hryn'ova,
W. R. Innes, M. H. Kelsey, P. Kim, D. W. G. S. Leith, S. Li, S. Luitz, V. Luth, H. L. Lynch,
D. B. MacFarlane, H. Marsiske, R. Messner, D. R. Muller, C. P. O'Grady, V. E. Ozcan, A. Perazzo,
M. Perl, T. Pulliam, B. N. Ratcliff, A. Roodman, A. A. Salnikov, R. H. Schindler, J. Schwiening,
A. Snyder, J. Stelzer, D. Su, M. K. Sullivan, K. Suzuki, S. K. Swain, J. M. Thompson, J. Va'vra, N. van

⁴Also at Laboratoire de Physique Corpusculaire, Clermont-Ferrand, France

Bakel, M. Weaver, A. J. R. Weinstein, W. J. Wisniewski, M. Wittgen, D. H. Wright, A. K. Yarritu, K. Yi,
C. C. Young

Stanford Linear Accelerator Center, Stanford, California 94309, USA

P. R. Burchat, A. J. Edwards, S. A. Majewski, B. A. Petersen, C. Roat, L. Wilden

Stanford University, Stanford, California 94305-4060, USA

S. Ahmed, M. S. Alam, R. Bula, J. A. Ernst, V. Jain, B. Pan, M. A. Saeed, F. R. Wappler, S. B. Zain

State University of New York, Albany, New York 12222, USA

W. Bugg, M. Krishnamurthy, S. M. Spanier

University of Tennessee, Knoxville, Tennessee 37996, USA

R. Eckmann, J. L. Ritchie, A. Satpathy, C. J. Schilling, R. F. Schwitters

University of Texas at Austin, Austin, Texas 78712, USA

J. M. Izen, X. C. Lou, S. Ye

University of Texas at Dallas, Richardson, Texas 75083, USA

F. Bianchi, F. Gallo, D. Gamba

Università di Torino, Dipartimento di Fisica Sperimentale and INFN, I-10125 Torino, Italy

M. Bomben, L. Bosisio, C. Cartaro, F. Cossutti, G. Della Ricca, S. Dittongo, L. Lanceri, L. Vitale

Università di Trieste, Dipartimento di Fisica and INFN, I-34127 Trieste, Italy

V. Azzolini, N. Lopez-March, F. Martinez-Vidal

IFIC, Universitat de Valencia-CSIC, E-46071 Valencia, Spain

Sw. Banerjee, B. Bhuyan, C. M. Brown, D. Fortin, K. Hamano, R. Kowalewski, I. M. Nugent, J. M. Roney,
R. J. Sobie

University of Victoria, Victoria, British Columbia, Canada V8W 3P6

J. J. Back, P. F. Harrison, T. E. Latham, G. B. Mohanty, M. Pappagallo

Department of Physics, University of Warwick, Coventry CV4 7AL, United Kingdom

H. R. Band, X. Chen, B. Cheng, S. Dasu, M. Datta, K. T. Flood, J. J. Hollar, P. E. Kutter, B. Mellado,
A. Mihalyi, Y. Pan, M. Pierini, R. Prepost, S. L. Wu, Z. Yu

University of Wisconsin, Madison, Wisconsin 53706, USA

H. Neal

Yale University, New Haven, Connecticut 06511, USA

1 INTRODUCTION

Detailed studies of the dynamics of semileptonic decays $D \rightarrow Ve^+\nu_e$, where V is a vector meson, have been performed for non-strange D mesons. It is expected that the corresponding semileptonic decay of the D_s meson, $D_s^+ \rightarrow \phi e^+\nu_e$,⁵ has similar properties. So far, measurements of this decay have been limited by the size of the available data sample. In this paper, we present a study of the hadronic form factors for the decay $D_s^+ \rightarrow \phi e^+\nu_e$ with $\phi \rightarrow K^+K^-$.

Neglecting the electron mass, the differential semileptonic decay rate of a scalar meson to a vector meson, specifically, $D_s^+ \rightarrow \phi e^+\nu_e$, depends on four variables [1] (see Figure 1),

- q^2 , the invariant mass squared of the e^+ and ν_e ;
- θ_e , the angle between the direction of the e^+ and the virtual W^+ , in the W^+ rest frame;
- θ_V , the angle between the direction of the K^- and the ϕ meson, in the ϕ rest frame;
- χ , the angle between the two decay planes of the W^+ and of the ϕ , in the D_s^+ rest frame. It corresponds to the angle between the directions of the e^+ and of the K^- , projected on a plane normal to the axis defined by the W^+/ϕ momentum in the D_s^+ rest frame. χ is defined in the range from $-\pi$ to $+\pi$.

It is assumed that ϕ decay to K^+K^- is well isolated from decays of other mesons to the same final state, and that any dependence of the rate on the variation of the K^+K^- invariant mass can be neglected.

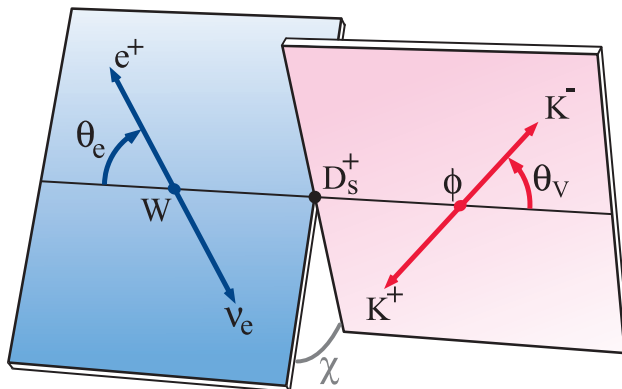


Figure 1: Definition of the angles θ_e , θ_V , and χ .

The differential decay rate can be written in terms of these variables as follows:

$$\frac{d^4\Gamma}{dq^2 d\cos\theta_V d\cos\theta_e d\chi} \propto p_\phi q^2 \begin{pmatrix} (1 + \cos\theta_e)^2 \sin^2\theta_V |H_+|^2 \\ + (1 - \cos\theta_e)^2 \sin^2\theta_V |H_-|^2 \\ + 4 \sin^2\theta_e \cos^2\theta_V |H_0|^2 \\ - 4 \sin\theta_e (1 + \cos\theta_e) \sin\theta_V \cos\theta_V \cos\chi H_+ H_0 \\ + 4 \sin\theta_e (1 - \cos\theta_e) \sin\theta_V \cos\theta_V \cos\chi H_- H_0 \\ - 2 \sin^2\theta_e \sin^2\theta_V \cos 2\chi H_+ H_- \end{pmatrix} \quad (1)$$

⁵Charge conjugate states are implied throughout this analysis.

where p_ϕ is the momentum of the ϕ meson in the rest frame of the D_s^+ . The helicity form factors can be written in the form

$$H_\pm(q^2) = (m_D + m_\phi)A_1(q^2) \mp 2\frac{m_D p_\phi}{m_D + m_\phi}V(q^2)$$

$$H_0(q^2) = \frac{1}{2m_\phi\sqrt{q^2}} \left[(m_D^2 - m_\phi^2 - q^2)(m_D + m_\phi)A_1(q^2) - 4\frac{m_D^2 p_\phi^2}{m_D + m_\phi}A_2(q^2) \right].$$

m_D and m_ϕ are the D_s^+ and ϕ masses, respectively. The vector and axial form factors are generally parameterized using an expression based on pole dominance [2]:

$$A_i(q^2) = \frac{A_i(0)}{1 - q^2/m_A^2} \quad (i = 1, 2), \quad V(q^2) = \frac{V(0)}{1 - q^2/m_V^2} \quad (2)$$

with the pole masses $m_A = 2.5 \text{ GeV}/c^2$ and $m_V = 2.1 \text{ GeV}/c^2$. These values are naive expectations assuming that the lower mass $c\bar{s}$ states with $J^P = 1^+$ and 1^- dominate the q^2 dependence of $A_{1,2}$ and V ⁶. It is expected that the simple pole ansatz has to be modified to include contributions from higher mass resonances in addition to the leading contribution. Measurements have usually been expressed in terms of the ratios of the form factors at $q^2 = 0$, namely:

$$r_V = V(0)/A_1(0) \quad \text{and} \quad r_2 = A_2(0)/A_1(0). \quad (3)$$

At present, there is no experimental determination of m_A and m_V .

It has been shown experimentally for the decay $D^0 \rightarrow K^- e^+ \nu_e$ [3] that the pole ansatz (Equation 2) using the nominal values of the D_s^* mass ($2.112 \text{ GeV}/c^2$) does not provide a good description of the q^2 dependence of the decay rate. A fit to data based on this ansatz results in a lower pole mass value, $m_V = 1.854 \pm 0.016 \pm 0.020 \text{ GeV}/c^2$.

Becirevic and Kaidalov [4] proposed a modification of the simple pole ansatz for the single form factor for semileptonic B and D mesons to pseudoscalar mesons. This proposed ansatz has been generalized [5] to describe B and D semileptonic decays to vector mesons. Specifically, the three form factors are parameterized as:

$$V(q^2) = \frac{c'_H(1-a)}{\left(1 - \frac{q^2}{m_{D_s^*}^2}\right) \left(1 - a\frac{q^2}{m_{D_s^*}^2}\right)}, \quad (4)$$

$$A_1(q^2) = \xi \frac{c'_H(1-a)}{\left(1 - b'\frac{q^2}{m_{D_s^*}^2}\right)}, \quad (5)$$

and

$$A_2(q^2) = \frac{c''_H}{\left(1 - b'\frac{q^2}{m_{D_s^*}^2}\right) \left(1 - b''\frac{q^2}{m_{D_s^*}^2}\right)}. \quad (6)$$

Based on this parameterization, r_V is a constant depending only on particle masses,

$$r_V = \frac{1}{\xi} = \frac{(m_{D_s} + m_\phi)^2}{m_{D_s}^2 + m_\phi^2} = 1.8. \quad (7)$$

⁶The 1^- state contributing to V is the D_s^* of mass $2.112 \text{ GeV}/c^2$, whereas the 1^+ states $D_{sJ}(2459)$ and $D_{s1}(2536)$ contribute to $A_{1,2}$

2 THE *BABAR* DETECTOR AND DATASET

The data used in this analysis were collected with the *BABAR* detector at the PEP-II storage rings operating at a center-of-mass (c.m.) energy optimized for $\Upsilon(4S)$ production. The *BABAR* detector is described in detail elsewhere [6].

This analysis is based on a fraction of the total available *BABAR* data sample, corresponding to integrated luminosities of 78.5 fb^{-1} recorded on the $\Upsilon(4S)$ resonance. Samples of Monte Carlo (MC) simulated $\Upsilon(4S) \rightarrow B\bar{B}$ decays, the production of charm- and light-quark pairs, equivalent to 4.1, 1.4 and 1.1 times the data statistics have been used to evaluate the efficiencies and background contributions. A dedicated sample of simulated signal events, with a uniform phase space distribution and equivalent to seven times the data, has been used to extract the fitted signal parameters.

3 ANALYSIS METHOD

This analysis focuses on semileptonic decays of D_s^+ mesons which are produced via $e^+e^- \rightarrow c\bar{c}$ annihilation. D_s mesons produced in $B\bar{B}$ events are not included and treated as background.

3.1 Candidate selection and background rejection

Fragmentation of the c and the \bar{c} quarks leads to the formation of two jets, back-to-back in the c.m. frame. In most cases, each jet contains one charm meson. The event thrust axis is determined from all charged and neutral particles measured in the c.m. system. To minimize the loss of particles close to the beam axis and to ensure a good reconstruction of the total energy and momentum in the event, we select events for which the direction of the thrust axis is in the interval $|\cos(\theta_{thrust})| < 0.75$.

Three variables, R_2 (the ratio of the second and zeroth order Fox-Wolfram moments [7]), the total multiplicity of charged and neutral particles, and the momentum of the fastest track in the event are used to reduce the contribution from $B\bar{B}$ events. These variables have been combined linearly to form a Fisher discriminant, \mathcal{F} . We choose a cut on \mathcal{F} that retains 68% of signal events and removes 70% of $B\bar{B}$ background.

A plane perpendicular to the thrust axis is used to define two hemispheres, equivalent to the two jets produced by quark fragmentation. In each hemisphere, we search for decay products of the D_s^+ , a charged lepton and two oppositely charged kaons. We use as charged leptons only positrons (or electrons for the charge conjugate D_s^- decays) with a c.m. momentum larger than $0.5 \text{ GeV}/c$.

Since the neutrino (ν_e) momentum is unmeasured, a kinematic fit is performed, constraining the invariant mass of the candidate ($e^+K^+K^-\nu_e$) system to the D_s^+ mass. In this fit, the D_s^+ momentum and the neutrino energy are estimated from the other particles measured in the event. The D_s^+ direction is taken as the direction opposite to the sum of the momenta of all reconstructed particles in the event, except for the two kaons and the positron associated with the signal candidate. The neutrino energy is estimated as the difference between the total energy of the jet and sum of the energies of all reconstructed particles in that hemisphere. The energy of the jet is determined from its mass and momentum. The jet mass is constrained taking into account that each jet contains at least one charm particle and thus its mass has to exceed the charm particle mass. The D_s^+ candidates are retained if the χ^2 probability of the kinematic fit exceeds 10^{-3} .

Tracks present in the signal hemisphere, which are not decay products of the D_s^+ candidate, are referred to as “spectator” (*spec*) tracks. Since the charm hadrons in a c or \bar{c} jet carry a large fraction of the jet energy, their decay products have on average higher energies than spectator particles. The following variables are used to define a second Fisher discriminant designed to select the signal $D_s^+ \rightarrow \phi e^+ \nu_e$ decays,

- the fitted D_s^+ momentum (P_{D_s});
- the mass of the spectator system ($m_{spec.}$);
- the direction of the spectator momentum relative to the thrust axis ($\cos(spec., thrust)$);
- the momentum of the leading spectator track ($P_{leading}$), i.e. the the spectator track having the largest momentum;
- the total momentum of the spectator system ($P_{spec.}$).

Figure 2 shows the K^+K^- invariant mass distribution for the selected decays compared to MC simulation and the composition of the background. We define ϕ candidates as K^+K^- pairs with an invariant mass in the interval from 1.01 and 1.03 GeV/ c^2 . We use a cut on the second Fisher discriminant that retains 64% of signal events and rejects 78% of combinatorial background. Of the background contribution of 26% in the signal region, 14 % are from continuum $q\bar{q}$ events (with $q = u, d, s$), 23.4 % are from $B^0\bar{B}^0$ events, 21.6 % from B^+B^- events, and the remainder are $c\bar{c}$ events. About 71% of the total background include a true ϕ decay combined with an electron from another source, namely B meson decays (41%), charm particle decays (25%), photon conversions or Dalitz decays (24%), and the rest are fake electrons. These ϕ mesons are expected to originate from the primary vertex, or from a secondary charm decay vertex.

3.2 Measurement of decay distributions

Taking into account the results of the kinematic fit, the decay rates are studied as a function of the following variables: q^2 (q_r^2), $\cos(\theta_e)$ ($\cos(\theta_e)_r$), $\cos(\theta_V)$ ($\cos(\theta_V)_r$) and χ (χ_r). Using simulated events, the resolution for these reconstructed variables has been studied by comparing the reconstructed (indicated by the index r) and true values.

The resolution functions have been fitted by the sum of two Gaussian distributions. The fitted standard deviations are listed in Table 1. This information is presented here to illustrate the performances of the reconstruction and the kinematic fit. The resolution parameters are not used in the fit to the decay distributions. Instead, the MC simulation uses the identical reconstruction of the four kinematic variables as used for the data, and thus the distributions of the simulated decays are expected to reproduce the data.

We have chosen a narrow interval in the K^+K^- invariant mass to select ϕ meson candidates. Any decay-rate variation as a function of the two-kaon mass is ignored.

3.3 Fitting procedure

We perform a maximum likelihood fit to the four-dimensional decay distribution in the variables q_r^2 , $\cos(\theta_V)_r$, $\cos(\theta_e)_r$ and χ_r using the likelihood function

$$\mathcal{L} = - \sum_{i=1}^{nbins} \ln \mathcal{P}(n_i^{\text{data}} | n_i^{\text{MC}}). \quad (8)$$

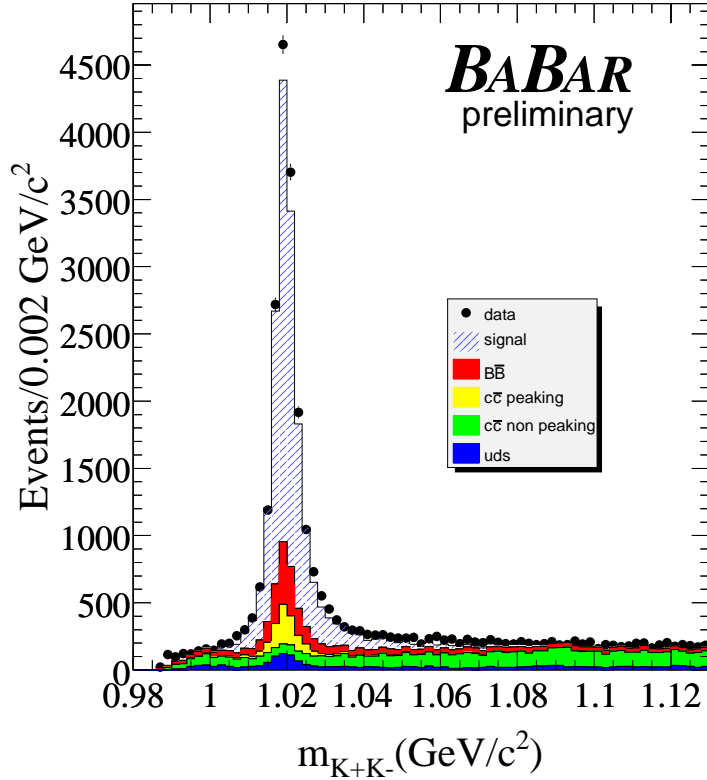


Figure 2: K^+K^- invariant mass distribution from data and simulated events. MC events have been normalized to the data luminosity according to the different cross sections. The excess of signal events in the ϕ region can be attributed to a different production rate and decay branching fraction of D_s^+ mesons in data and in simulated events. Dedicated studies have been done to evaluate the amount of peaking background in real events.

Table 1: Resolution of the reconstructed four kinematic variables: Standard deviations of the two Gaussian distributions, and their relative contribution.

variable	σ_1	σ_2	fraction of the narrower Gaussian
q^2	0.0778 GeV ²	0.249 GeV ²	0.33
$\cos(\theta_e)$	0.046	0.228	0.47
$\cos(\theta_V)$	0.099	0.387	0.43
χ	0.262 rad	1.39 rad	0.41

In this expression, for each bin i , $\mathcal{P}(n_i^{\text{data}}|n_i^{\text{MC}})$ is the Poisson probability to observe n_i^{data} events, when n_i^{MC} are expected. Considering the typical resolutions given in Table 1 and the available statistics, we have chosen five bins for each of the four variables, corresponding a four-dimensional array with a total of $\text{nbins} = 625$.

The expected number of events results from:

- combinatorial background in the ϕ signal interval;
- peaking background, i.e. real ϕ decays combined with a background electron;
- $\phi e^+ \nu_e$ signal events.

The number of expected signal events is obtained from MC simulation in the following way. A dedicated sample of signal events is generated with a uniform decay phase space distribution, and each event is weighted using the differential decay rate given in Equation 1, divided by p_ϕ .

We take advantage of the fact that the estimated background rate is flat in two of the four variables, $\cos(\theta_V)$ and χ (see Figure 3), by averaging over these distributions,

$$n_{i_{q^2, i_{\cos(\theta_e)}, i_{\cos(\theta_V)}, i_\chi}}^{\text{bckg.}} = \frac{\sum_{j,k=1}^{\text{nbins}_{\cos(\theta_V)}, \text{nbins}_\chi} n_{i_{q^2, i_{\cos(\theta_e)}, j, k}}^{\text{bckg.}}}{\text{nbins}_{\cos(\theta_V)} \text{nbins}_\chi} \quad (9)$$

This expression applies to each component of background. The background components are normalized to correspond to the expected rates for the integrated luminosity of the data sample.

The absolute normalization for signal events (N_S) is left free to vary in the fit. In each bin (i), the expected number of events is evaluated to be:

$$n_i^{\text{MC}} = N_S \frac{\sum_{j=1}^{n_i^{\text{signal}}} w_j(\lambda_k)}{W_{\text{tot}}(\lambda_k)} + n_i^{\text{bckg.}} \quad (10)$$

Here n_i^{signal} refers to the number of simulated signal events, with reconstructed values of the four variables corresponding to bin i . The weight w_j is evaluated for each event, using the generated values of the kinematic variables, thus accounting for resolution effects. $W_{\text{tot}}(\lambda_k) = \sum_{j=1}^{N^{\text{signal}}} w_j(\lambda_k)$ is the sum of the weights for all simulated signal events which have been generated according to a uniform phase space distribution. N_S and λ_k are the parameters to be fitted. Specifically, the free parameters λ_k are r_V , r_2 , and parameters which define q^2 dependence of the form factors. To avoid having to introduce finite ranges for the fit to the pole masses, m_i , we define $m_i = 1 + \lambda_i^2$. This expression ensures that m_i is always larger than $q_{\text{max}}^2 \simeq 0.9 \text{ GeV}^2$.

4 RESULTS OF THE FIT TO THE DECAY RATE

The fit to the four-dimensional data distribution is performed using simulated signal events generated according to a uniform phase space distribution. Signal MC events are weighted to correct for differences in the quark fragmentation process between data and simulated events. Using fixed values for the pole masses ($m_A = 2.5 \text{ GeV}/c^2$ and $m_V = 2.1 \text{ GeV}/c^2$) the following results are obtained:

$$N_S = 12886 \pm 129, \quad r_V = 1.636 \pm 0.067, \quad r_2 = 0.705 \pm 0.056.$$

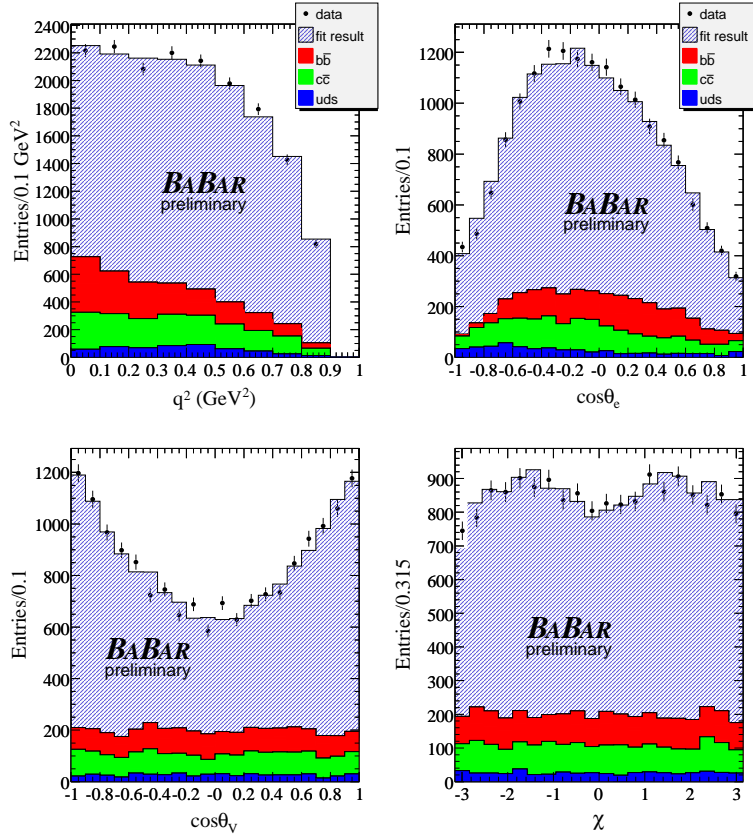


Figure 3: Projected distributions of the reconstructed four kinematic variables which define the decay rate for $D_s^+ \rightarrow \phi e^+ \nu_e$. The data (with statistical errors) are compared to histograms showing size of the fitted signal and background contributions.

The measured distributions, projected on the four variables, are compared with the results of the fit in Figure 3. The fit procedure has been verified with fits to a large number of simulated toy experiments with event samples of comparable size.

If we keep m_V fixed, the pole mass for the vector form factor, for which there is no sensitivity, and leave m_A , the pole mass of the axial vector form factor, as a free parameter, we obtain

$$N_S = 12887 \pm 129, \quad r_V = 1.633 \pm 0.081, \quad r_2 = 0.711 \pm 0.111, \quad m_A = (2.53_{-0.35}^{+0.54}) \text{ GeV}/c^2.$$

5 SYSTEMATIC STUDIES

The following sources of systematic uncertainties have been considered.

5.1 Generator tuning

The fraction of the beam energy carried by a D_s^+ meson is rather different in data and MC simulation. This difference has been measured using $D_s^+ \rightarrow \phi\pi^+$ decays. After applying this correction, there remain small differences in the distributions of the variables entering the Fisher discriminant, used to reduce the background level. These differences have been evaluated using also samples of $D_s^+ \rightarrow \phi\pi^+$ decays. The largest of the remaining differences results in the following changes of the fitted parameters,

$$\delta(N_S) = +5, \quad \delta(r_V) = -0.005, \quad \delta(r_2) = +0.008. \quad (11)$$

For the second fit with variable pole mass, m_A , these changes are:

$$\delta(N_S) = +3, \quad \delta(r_V) = +0.008, \quad \delta(r_2) = -0.017, \quad \delta(m_A) = -0.10 \text{ GeV}/c^2. \quad (12)$$

5.2 Background control

Two contributions have to be considered:

5.2.1 Combinatorial background

The level of combinatorial background has been evaluated using the mass intervals $1.10 < m_{KK} < 1.15 \text{ GeV}/c^2$, where the contributions from true $\phi \rightarrow K^+K^-$ decays are negligible. In this region we found an excess of 7% in data over MC simulated events. We assign a 10% uncertainty to the combinatorial background estimate. The corresponding systematic uncertainties on r_V and r_2 are:

$$\delta(r_V) = \pm 0.008, \quad \delta(r_2) = \pm 0.003.$$

For the second fit with variable pole mass, m_A , these uncertainties are:

$$\delta(r_V) = \pm 0.022, \quad \delta(r_2) = \pm 0.032, \quad \delta(m_A) = \pm 0.114 \text{ GeV}/c^2.$$

5.2.2 Background from ϕ mesons produced in D or B decays

The rate of these background sources depends on branching fractions to ϕ mesons. A study has been performed to compare the ϕ meson production rate in data and simulated events using different event samples which have been normalized to the same integrated luminosity. Events with a candidate electron and a candidate ϕ are used since they correspond to a sample enriched in charm decays. The production of a ϕ meson is studied, in the same hemisphere that contains the lepton, and in the other.

The production of ϕ mesons in remaining $B\bar{B}$ background has been measured by subtracting off-peak from on-peak events ⁷. From comparisons of data and MC simulated $B\bar{B}$ samples, we conclude that the simulation provides a description of ϕ production, accompanying a lepton, with an accuracy better than 10%.

The production of ϕ mesons accompanied by an electron has been also studied using off-peak events. These events have contributions from c and u, d, s quark-pair production. Correction factors, to be applied to the simulated ϕ rate, are determined such that the total expected ϕ production and the fractions expected from c - and u, d, s events agree with data. The values are given in Table 2. We assign a systematic uncertainty of $\pm 10\%$ to these corrections.

Table 2: Correction factors to be applied on the simulated ϕ production rate in $e^+e^- \rightarrow q\bar{q}$.

quark	ϕ accompanying the lepton	ϕ opposite the lepton
c	0.85	0.80
uds	1.06	1.05

Background events from $D_s^+ \rightarrow \phi\pi^0 e^+\nu_e$ decays can have decay characteristics that differ slightly from the signal decays. The ϕ and the positron originate from the same D_s^+ hadron, contrary to other peaking background sources. But the rate for this decay is suppressed by the OZI rule, and the detection efficiency is expected to be lower than for the signal events. In the following, its contribution is neglected.

Considering $\pm 10\%$ uncertainties on the B and D peaking background, the corresponding systematic uncertainties on r_V and r_2 are:

$$\delta(r_V) = \pm 0.019, \quad \delta(r_2) = \pm 0.009.$$

If, in addition, m_A has been fitted, the uncertainties are:

$$\delta(r_V) = \pm 0.052, \quad \delta(r_2) = \pm 0.072, \quad \delta(m_A) = \pm 0.48 \text{ GeV}/c^2.$$

5.3 Monte Carlo statistics

In the fitting procedure two sources of statistical fluctuations are not included. They originate from the finite statistics of the weighting procedure applied to simulated signal events and from

⁷On-peak events are recorded at the $\Upsilon(4S)$ energy whereas off-peak events are recorded at an energy 40 MeV below.

uncertainties in the estimate of the average number of background events in each bin. As a result, statistical uncertainties obtained from the standard fits to data or simulated events may be underestimated and the values of the fitted parameters may have biases.

The effect of these statistical errors on the fitted parameters r_V and r_2 have been evaluated using 1000 simulated toy fits. For each toy fit, not only the “fake experiment” is generated, but also the sample of pure signal and the background distributions are created. In each of these experiments, the same number of signal events (13 000) and the same ratio background over signal, B/S=0.31 as the data is used. The predicted distributions in the fit are generated uniformly over the decay phase space, with samples of 110,000 events each, as in the real fit. The width of the normalized pull distributions of the toy fits is 1.07 and the bias is 0.08. Uncertainties on these numbers are ± 0.03 . The systematic uncertainty attached to possible biases is assumed to be $0.1 \times \sigma_{\text{fit}}$, where σ_{fit} is the statistical uncertainty of the fit. The uncertainty assigned to the size of the simulated events sample and to the statistical uncertainties on the average number of background events in each bin, is estimated from the increase of the width of the pull distribution relative to unity:

$$\sqrt{1.1^2 - 1} \times \sigma_{\text{fit}} \simeq 0.46 \times \sigma_{\text{fit}}, \quad (13)$$

where 0.1 is chosen as the upper limit for the observed deviations.

5.4 Remaining detector effects

Effects induced by momentum dependent differences on the electron and charged kaon reconstruction efficiency between data and simulated events have been evaluated. Standard correction factors determined from selected control data samples, have been applied to correct for these differences which are typically of a few percent. The impact of this correction on the fitted parameters are:

$$\delta(r_V) = +0.018, \quad \delta(r_2) = +0.012.$$

If, in addition, m_A is fitted, the variations are:

$$\delta(r_V) = +0.017, \quad \delta(r_2) = +0.015, \quad \delta(m_A) = +0.02 \text{ GeV}/c^2.$$

The systematic uncertainty of these corrections is estimated to be 30% and corresponding values have been given in Tables 3 and 4 respectively.

5.5 Reconstruction accuracy on the kinematic variables

Using $D^{*+} \rightarrow D^0 \pi^+$ and $D^0 \rightarrow K^- \pi^+ \pi^0$ events it has been verified that differences between data and simulated events in the resolution of the variables q^2 and $\cos(\theta_e)$ are small compared with other sources of systematic uncertainties. They have been neglected at present.

5.6 Summary of systematic uncertainties

A summary of the systematic uncertainties on the measurement of r_V and r_2 is given in Table 3 and in Table 4, for fits that include m_A as a free parameter.

Table 3: Systematic uncertainties on r_V and r_2 .

Source	error on r_V	error on r_2
Generator tuning	0.005	0.008
Background control	0.021	0.009
Monte-Carlo statistics	0.031	0.026
Detector effects	0.006	0.004
Total	0.038	0.029

Table 4: Systematic uncertainties on r_V , r_2 and m_A .

Source	error on r_V	error on r_2	error on m_A (GeV/ c^2)
Generator tuning	0.008	0.017	0.10
Background control	0.056	0.079	0.49
Monte-Carlo statistics	0.038	0.052	0.21
Detector effects	0.006	0.005	0.01
Total	0.068	0.096	0.54

6 RESULTS AND CONCLUSIONS

Assuming pole dominance for the different form factors and using the fixed pole mass values, the contributions of the A_2 and V hadronic form factors, relative to A_1 , have been measured in a sample of 13,000 $D_s^+ \rightarrow \phi e^+ \nu_e$ decays. In this measurement, pole mass expressions have been used for the q^2 dependence of the form factors and values for the pole masses, equal to those assumed in previous experiments have been used. We have obtained:

$$r_V = V(0)/A_1(0) = 1.636 \pm 0.067 \pm 0.038 \text{ and } r_2 = A_2(0)/A_1(0) = 0.705 \pm 0.056 \pm 0.029$$

where the first uncertainty is statistical, and the second is systematic. These values are compatible with and more accurate than previous determinations.

The present measurement has a limited sensitivity on m_V and its value has been fixed at 2.1 GeV/ c^2 . Allowing the pole mass of the axial form factors, m_A , to vary as a free parameter in the fit, we obtain

$$r_V = V(0)/A_1(0) = 1.633 \pm 0.081 \pm 0.068, \quad r_2 = A_2(0)/A_1(0) = 0.711 \pm 0.111 \pm 0.096$$

$$\text{and } m_A = (2.53_{-0.35}^{+0.54} \pm 0.54) \text{ GeV}/c^2.$$

The fitted value of m_A agrees with the assumed default value.

In Table 5, the results of this analysis are compared with earlier measurements obtained in photoproduction experiments at Fermilab [8, 9, 10, 11] and by the CLEOII experiment [12]. The central values and corresponding total errors are also shown in Figure 4.

The measurements of the parameters r_V and r_2 for the semileptonic decay $D_s^+ \rightarrow \phi e^+ \nu_e$ now have an accuracy similar to the one obtained for $D \rightarrow K^* e^+ \nu_e$ decays [13]. This allows meaningful comparisons for the first time, see Table 6 and Figure 4. Measurements of r_V for the two decays

Table 5: Results from previous experiments and present measurements. They have been obtained assuming a pole mass dependence for the hadronic form factors with fixed values of the pole masses: $m_A = 2.5 \text{ GeV}/c^2$ and $m_V = 2.1 \text{ GeV}/c^2$.

Experiment	Statistics (S/B)	r_V	r_2
E653 [8]	19/5	$2.3^{+1.1}_{-0.9} \pm 0.4$	$2.1^{+0.6}_{-0.5} \pm 0.2$
E687 [9]	90/33	$1.8 \pm 0.9 \pm 0.2$	$1.1 \pm 0.8 \pm 0.1$
CLEOII [12]	308/166	$0.9 \pm 0.6 \pm 0.3$	$1.4 \pm 0.5 \pm 0.3$
E791 [10]	$\sim 300/60$	$2.27 \pm 0.35 \pm 0.22$	$1.57 \pm 0.25 \pm 0.19$
FOCUS [11]	$\sim 560/250$	$1.549 \pm 0.250 \pm 0.145$	$0.713 \pm 0.202 \pm 0.266$
<i>BABAR</i>	12972/3931	$1.636 \pm 0.067 \pm 0.038$	$0.705 \pm 0.056 \pm 0.029$

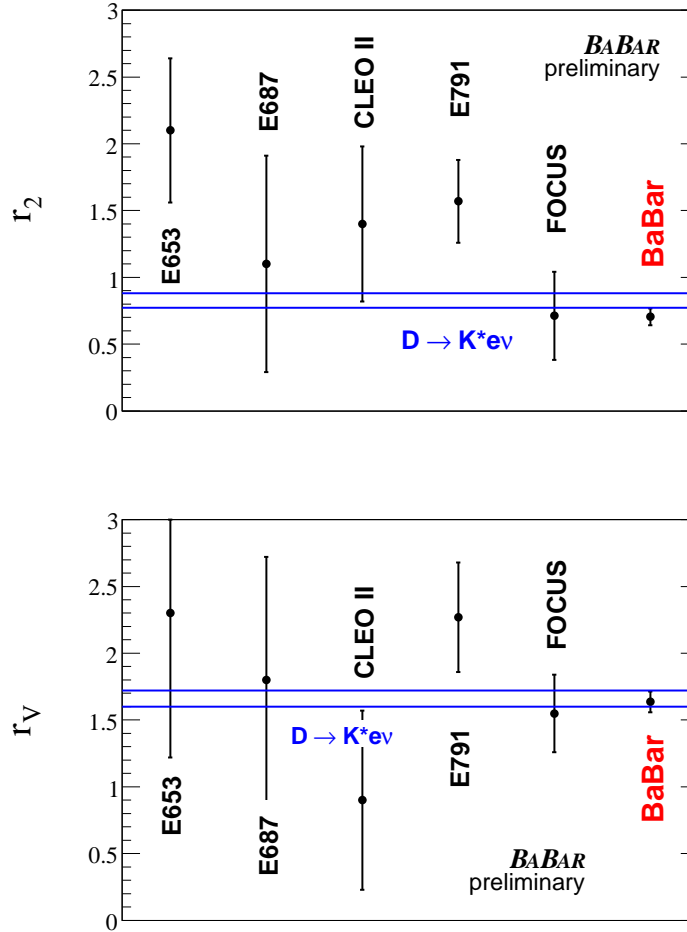


Figure 4: Results from previous experiments and present measurement of r_2 and r_V in $D_s^+ \rightarrow \phi e^+ \nu_e$ decays. The error bars represent the statistical and systematic uncertainties added in quadrature. These measurements for $D_s \rightarrow \phi e^+ \nu_e$ decays are compared with the average of similar measurements obtained for $D \rightarrow K^* e^+ \nu_e$ decays. The \pm one sigma range is indicated by the two parallel lines.

are in full agreement within the experimental uncertainties. This was expected theoretically, given the parameterization of Equation 7. However, the measured value is lower than the expectation of 1.8. Values for r_2 differ by 1.5σ between the two decay modes.

Table 6: Comparison between $D/D_s^+ \rightarrow Ve^+\nu_e$ decays.

Parameter	$D_s^+ \rightarrow \phi e^+ \nu_e$ (this analysis)	$D \rightarrow K^* e^+ \nu_e$ (average value at FPCP06)
r_V	$1.636 \pm 0.067 \pm 0.038$	1.66 ± 0.06
r_2	$0.705 \pm 0.056 \pm 0.029$	0.827 ± 0.055

7 ACKNOWLEDGMENTS

We are grateful for the extraordinary contributions of our PEP-II colleagues in achieving the excellent luminosity and machine conditions that have made this work possible. The success of this project also relies critically on the expertise and dedication of the computing organizations that support *BABAR*. The collaborating institutions wish to thank SLAC for its support and the kind hospitality extended to them. This work is supported by the US Department of Energy and National Science Foundation, the Natural Sciences and Engineering Research Council (Canada), Institute of High Energy Physics (China), the Commissariat à l’Energie Atomique and Institut National de Physique Nucléaire et de Physique des Particules (France), the Bundesministerium für Bildung und Forschung and Deutsche Forschungsgemeinschaft (Germany), the Istituto Nazionale di Fisica Nucleare (Italy), the Foundation for Fundamental Research on Matter (The Netherlands), the Research Council of Norway, the Ministry of Science and Technology of the Russian Federation, Ministerio de Educación y Ciencia (Spain), and the Particle Physics and Astronomy Research Council (United Kingdom). Individuals have received support from the Marie-Curie IEF program (European Union) and the A. P. Sloan Foundation.

References

- [1] G.Kopp, G. Kramer, G.A. Schuler and W.F. Palmer, *Z. Phys. C* **48**, 327 (1990).
- [2] J.G. Koerner and G.A. Schuler, *Z. Phys. C* **38**, 511 (1988); Erratum-ibid *C* **41**, 690 (1989).
M. Bauer and M. Wirbel, *Z. Phys. C* **42**, 671 (1989).
- [3] B. Aubert *et al.*, *BABAR* Collaboration, *BABARCONF-06/006*, SLAC-PUB-0000, hep-ex/0000, submitted to the 33rd International Conference on High-Energy Physics, ICHEP 06, 26 July - 2 August 2006, Moscow, Russia, and references therein.
- [4] D. Becirevic and A.B. Kaidalov, *Phys. Lett. B* **478**, 417 (2000) [arXiv:hep-ph/9904490].
- [5] S.Fajfer and J. Kamenik, *Phys. Rev. D* **72**, 034029 (2005) [arXiv:hep-ph/0506051] and [arXiv:hep-ph/0601028].
- [6] B. Aubert *et al.*, *BABAR* Collaboration *Nucl. Instrum. Methods A* **479**, 1 (2002).
- [7] G. C. Fox and S. Wolfram, *Phys. Rev. Lett.* **41**, 1581 (1978).

- [8] K. Kodama *et al.*, E653 Collaboration, Phys. Lett. B **309**, 483 (1993).
- [9] P. L. Frabetti *et al.*, E687 Collaboration, Phys. Lett. B **328**, 187 (1994).
- [10] E.M. Aitala *et al.*, E791 Collaboration, Phys. Lett. B **450**, 294 (1999) [arXiv:hep-ex/9812013].
- [11] J.M. Link *et al.*, FOCUS Collaboration, Phys. Lett. B **586**, 183 (2004) [arXiv:hep-ex/0401001].
- [12] P. Avery *et al.* , CLEO Collaboration, Phys. Lett. B **337**, 405 (1994).
- [13] J. Wiss, “Recent results on fully leptonic and semileptonic charm decays”, FPCP Conference, Vancouver 2006 [arXiv:hep-ex/0605030].